Neurosci Bull June 1, 2013, 29(3): 279–286. http://www.neurosci.cn
DOI: 10.1007/s12264-013-1333-z

·Original Article·

Encoding of rat working memory by power of multi-channel local field potentials *via* sparse non-negative matrix factorization

Xu Liu[1], Tiao-Tiao Liu[2], Wen-Wen Bai[2], Hu Yi[2], Shuang-Yan Li[1], Xin Tian[1,2]
[1]*School of Biomedical Engineering, Tianjin Medical University, Tianjin 300070, China*
[2]*Research Center of Basic Medicine, Tianjin Medical University, Tianjin 300070, China*
Corresponding author: Xin Tian. E-mail: tianx@tmu.edu.cn

ABSTRACT

Working memory plays an important role in human cognition. This study investigated how working memory was encoded by the power of multi-channel local field potentials (LFPs) based on sparse non-negative matrix factorization (SNMF). SNMF was used to extract features from LFPs recorded from the prefrontal cortex of four Sprague-Dawley rats during a memory task in a Y maze, with 10 trials for each rat. Then the power-increased LFP components were selected as working memory-related features and the other components were removed. After that, the inverse operation of SNMF was used to study the encoding of working memory in the time-frequency domain. We demonstrated that theta and gamma power increased significantly during the working memory task. The results suggested that postsynaptic activity was simulated well by the sparse activity model. The theta and gamma bands were meaningful for encoding working memory.

Keywords: sparse non-negative matrix factorization; multi-channel local field potentials; working memory; prefrontal cortex

INTRODUCTION

Working memory refers to a brain system that provides temporary storage and manipulation of information, supporting human thought processes by providing an interface between perception, long-term memory and action[1-3]. Studies have suggested that working memory is mediated by the continuous activity of prefrontal cortex (PFC) neurons[4,5], and the PFC plays an important role in working memory[6,7]. Multi-channel local field potentials (LFPs) are signals recorded from extracellular electrodes that result from superposition of local excitatory and inhibitory postsynaptic potentials[8]. LFPs recorded from the PFC are rich in information related to working memory[9,10]. One study has shown that theta (4–12 Hz) oscillations peak at the choice point when rats execute Y-maze tasks[11]. Gamma (30–80 Hz) oscillations also play an important role in functions such as information transmission and storage[12-14].

However, not all components of LFPs recorded from the PFC are devoted to encoding working memory. It would therefore be beneficial to remove the noise for intensive studies of working memory. The conventional methods for analyzing LFPs include principal component analysis, independent component analysis, factor analysis and non-negative matrix factorization (NMF), among which only NMF can ensure non-negative decomposition. Since the LFP power is non-negative, NMF has certain advantages in analyzing these signals. Moreover, considering the sparseness of neuronal activity[15], we gave the NMF algorithm a sparseness constraint to better simulate neuronal activity. So in this study, sparse non-negative matrix factorization (SNMF) was used to extract features from the time-frequency representation of LFPs.

The power in the theta and gamma bands has been reported to increase during working memory[16-19]; based on this, we selected the power-increased LFP components as working memory-related features and eliminated the other components. After that, the inverse operation of SNMF was used to reconstruct working memory-related features. Then we obtained the time-frequency representation of the power-increased LFP power components, which are useful for studying working memory.

MATERIALS AND METHODS

All surgical and experimental procedures conformed to the Guidelines for the Care and Use of Laboratory Animals and were approved by the Tianjin Medical University Animal Care and Use Committee.

Training and Data Acquisition

LFPs were recorded from the PFC of male Sprague-Dawley rats (300–350 g, 17 weeks old) during a Y-maze working memory task (Fig. 1). Each trial consisted of a free choice and a delayed alternation. After raising the guillotine door, the rat started the free choice from arm A. The rat would get a small piece of food as a reward when it chose either arm B or arm C. Then the rat returned to the starting point (arm A), and the door was lowered. After a 5-s interval, the door was raised again and the rat started a 'choice run'. If the rat reached the end of the arm that was not chosen previously, it would get a food reward. After each trial, the animal returned to arm A to start the next trial (Fig. 1).

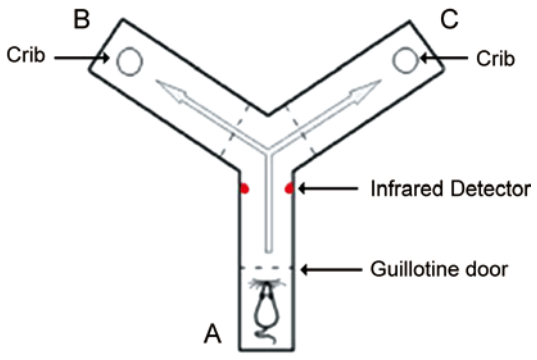

Fig. 1. Schematic representation of the Y maze. Arm A is the starting position. Cribs for reward delivery are located at the ends of arms B and C.

Before training in the Y-maze, the rats had free access to water and 2 days of food restriction. We limited the access to food to 2 h/day and adjusted the quantity to maintain body weight at a minimum of 85% of normal body weight under a normal 12 h light-12 h dark cycle.

The rats received training sessions until their performance reached a steady rate of at least 80% correct. Under aseptic conditions and chloral hydrate (350 mg/kg) anesthesia, the rats were then implanted with a 16-channel nickel-cadmium microelectrode array (impedance <1 MΩ) targeting the PFC (AP: 2.5–4.5 mm, ML: 0.2–1.0 mm, DL: 2.5–3.5 mm). The array location was estimated *in vivo* using a stereotaxic instrument and a drive to calculate the depth. After recovery, the raw signals were recorded during training sessions with a Cerebus Data Acquisition System (Cyberkinetics, Foxborough, MA). LFPs (low-pass filter, 0.3–500 Hz) sampled at 2 000 Hz were extracted from the raw signals *via* digital filters in the Neural Signal Processor (Fig. 2).

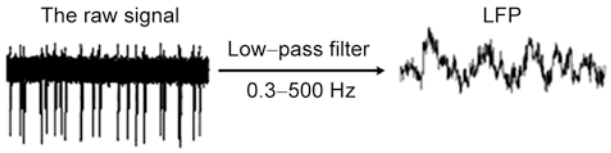

Fig. 2. The LFP (low-pass filter, 0.3–500 Hz) sampled at 2 000 Hz was extracted from the raw signal *via* digital filters in the Neural Signal Processor.

Working Memory Group

When rats made a choice run, the occurrence of behavioral events was marked using an infrared detector in the Y maze (Fig. 1), crossing of which defined as the 'reference point' (RP). The duration of each LFP used in this study was 6 s (4 s before and 2 s after the RP), which included the process of the working memory event.

Control group

Before the working memory task, the rat was placed at A arm and left for ~5 min with the guillotine door closed, when LFPs were recorded as controls.

SNMF for Spectral LFP Feature Extraction

Given a non-negative matrix $\boldsymbol{X}_{m\times n}$, a natural number r < min

(m, n), and parameter λ, SNMF seeks the non-negative matrices $\boldsymbol{A}_{m\times r}$ and $\boldsymbol{S}_{r\times n}$. According to the principle of sparse coding[20], the objective function of SNMF can be written as:

$$D(\boldsymbol{X},\boldsymbol{AS})=\sum_{i,j}\left\{\boldsymbol{X}_{ij}\log\frac{\boldsymbol{X}_{ij}}{(\boldsymbol{AS})_{ij}}-\boldsymbol{X}_{ij}+(\boldsymbol{AS})_{ij}\right\}+\lambda\sum_{k,j}\boldsymbol{S}_{k,j} \quad (1)$$

where λ >0. The parameter λ balances the trade-off between the accuracy of approximation and the sparseness of $\boldsymbol{S}$. A larger value of λ implies stronger sparsity while smaller values of λ can be used for better accuracy of approximation[21]. The columns of matrix $\boldsymbol{A}$ are normalized to unit L_2-norm here[22]. Using a gradient-based search to minimize this divergence with a step-size yielding multiplicative updates, the following updates of $\boldsymbol{A}$ and $\boldsymbol{S}$ forming the NMF-KL algorithm are achieved[23]:

$$\begin{aligned}&\boldsymbol{A}_{ik}\leftarrow\boldsymbol{A}_{ik}\textstyle\sum_j\boldsymbol{S}_{kj}\boldsymbol{X}_{ij}\big/(\boldsymbol{AS})_{ij},\\&\boldsymbol{A}_{ik}\leftarrow\boldsymbol{A}_{ik}\big/\textstyle\sum_l\boldsymbol{A}_{lk},\\&\boldsymbol{S}_{kj}\leftarrow\frac{\boldsymbol{S}_{kj}\sum_i\boldsymbol{A}_{ik}\boldsymbol{X}_{ij}/(\boldsymbol{AS})_{ij}}{1+\lambda}.\end{aligned} \quad (2)$$

We constructed the data matrix $\boldsymbol{X}\in\boldsymbol{R}_{+}^{m\times n}$ from the time-domain of the LFP data. After removing the baseline, a short-time Fourier transform (Hamming window length, 3 000; step size, 1; number of frequency samples, 1 024) was used to obtain the time-frequency representation of the LFP, which we denoted by $\boldsymbol{P}_{t,f}^{k}\in\boldsymbol{R}^{F\times n}$. Then we constructed the data matrix $\boldsymbol{X}$ by $\boldsymbol{P}_{t,f}^{k}$ as:

$$\boldsymbol{X}=[\boldsymbol{P}_{t,f}^{1};\boldsymbol{P}_{t,f}^{2};...;\boldsymbol{P}_{t,f}^{K}]\in\boldsymbol{R}^{m\times n} \quad (3)$$

where channel, time and frequency indices respectively run over k = 1 ,…, K, t = 1 ,…, n, and f = 1 ,…, F, and $m = K \times F$. We took the number of frequency indices F as 42 to keep the frequency below 80 Hz and the number of time indices n = 12 000. An application of SNMF to two-channel LFP data is shown in Fig. 3. The data matrix $\boldsymbol{X}$ is decomposed into a product of basis matrix $\boldsymbol{A}$ and sparse matrix $\boldsymbol{S}$. Basis matrix $\boldsymbol{A}$ contains bases in its columns, which we took as different types of postsynaptic potentials, and each row of sparse matrix $\boldsymbol{S}$ shows how each basis varies with time.

In SNMF, the values of parameters r and λ must be set. Different parameter values lead to different results. Researchers often set reasonable values of the parameters according to their own experience, or by numerical pretreatment[24-26]. Considering the accuracy of approximation and the sparseness of $\boldsymbol{S}$, the parameters r and λ were chosen to be 40 and 0.6 respectively after repeated tests.

Selection and Reconstruction of Working Memory-Related Features

Based on elevations in LFP power[16-19], we selected working memory-related features. First, we determined the approximate time of the working memory event from matrix $\boldsymbol{S}$. Let H_i be the maximum value of each row vector $\boldsymbol{S}_i$ in the time we determined before, and G the maximum value of H_i. If $H_i > 0.3G$, then we selected the corresponding row vector $\boldsymbol{S}_i$ as the working memory-related row vector, which was denoted F_i. Then we set the other rows of matrix $\boldsymbol{S}$ to 0. After that we obtained a new matrix $\boldsymbol{U}$ from matrix $\boldsymbol{S}$. Finally we reconstructed features using the inverse operation of SNMF as:

$$\boldsymbol{Y}=\boldsymbol{AU} \quad (4)$$

where $\boldsymbol{Y}$ contains the time-frequency information of the working memory-related features. Then the purpose of removing noise was achieved. An application of reconstruction is shown in Fig. 4.

RESULTS

In this study, LFPs were recorded from the PFC of four rats during the Y-maze working memory task, with 10 trials for each rat. LFPs from one rat were 15-channel data, while those from the other three were all 16-channel data. The length of each data segment was 6 s (4 s before and 2 s after the RP), which included the entire process of working memory events.

Theta and Gamma Power Changes during Working Memory

Examples of LFP and time-frequency representation in the working memory and control groups were shown in Fig. 5A and B. We analyzed the changes of theta and gamma power over time in the working memory and control groups (Fig. 5C, D) and found that there were no significant differences in the theta and gamma power in each corresponding second between two groups. LFP power increased remarkably in a specific period of the alternate

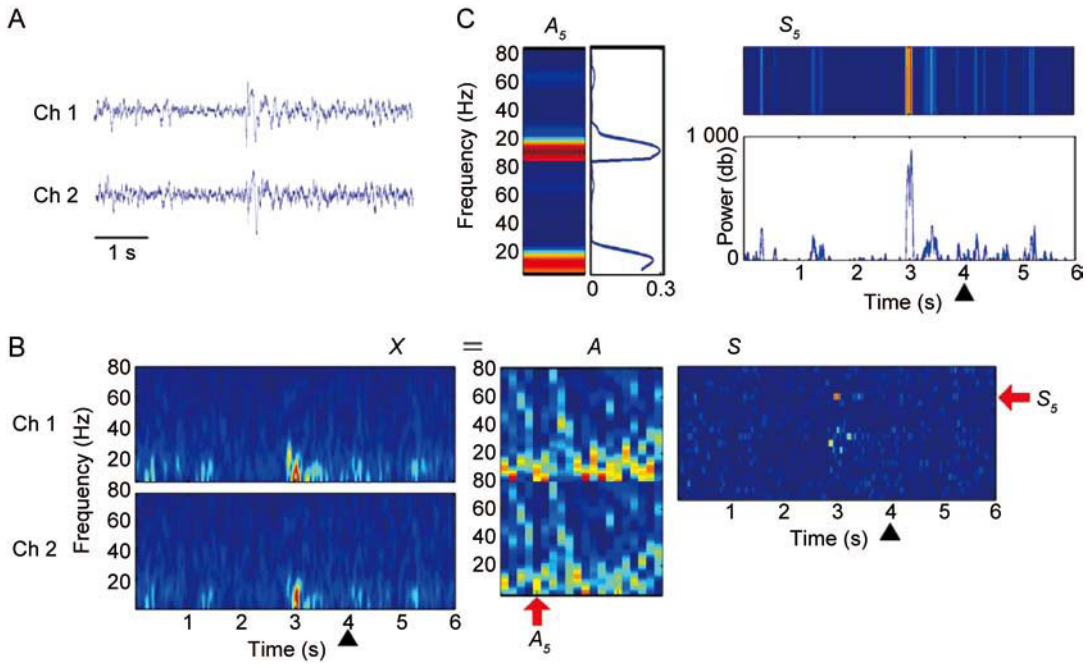

Fig. 3. Application of SNMF to two-channel LFP data. A: The two-channel time-domain LFP data after removing the baseline. B: The data matrix *X* constructed with two-channel time-domain LFP data is decomposed into a product of basis matrix *A* and sparse matrix *S*. The vertical axis of matrix *A* represents frequencies between 0 and 80 Hz in each channel, and the horizontal axis is related to the number of basis vectors. The vertical axis of matrix *S* is related to the number of sparse vectors, and the horizontal axis represents time. C: Basis vector A_5 is mainly related to the theta band for channels 1 and 2. Sparse vector S_5 shows the power of the corresponding feature concentrates near 3 s. Symbol ▲ denotes the reference point.

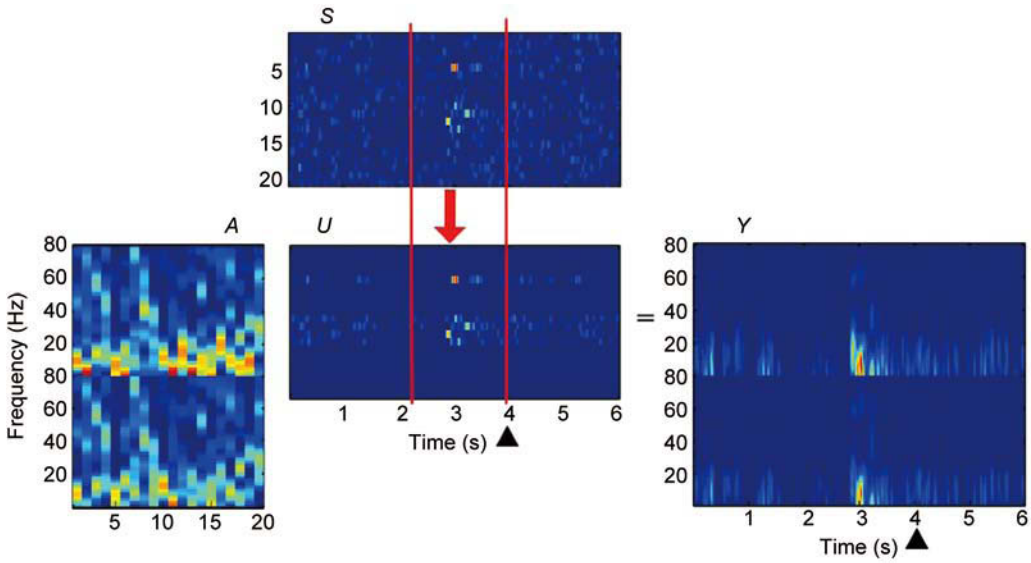

Fig. 4. Diagram of the principle of selection and reconstruction of working memory-related features. The power of some sparse vectors remarkably increased in the time period between the red lines, while the power of the other vectors was almost invariant. The features whose power remarkably increased were selected as working memory-related features. Matrix *U* obtained from matrix *S* contained many 0 vectors that were not working memory-related features. Matrix *Y*, which was derived from matrices *A* and *U*, contained the time-frequency information of the working memory-related features. ▲ denotes the reference point.

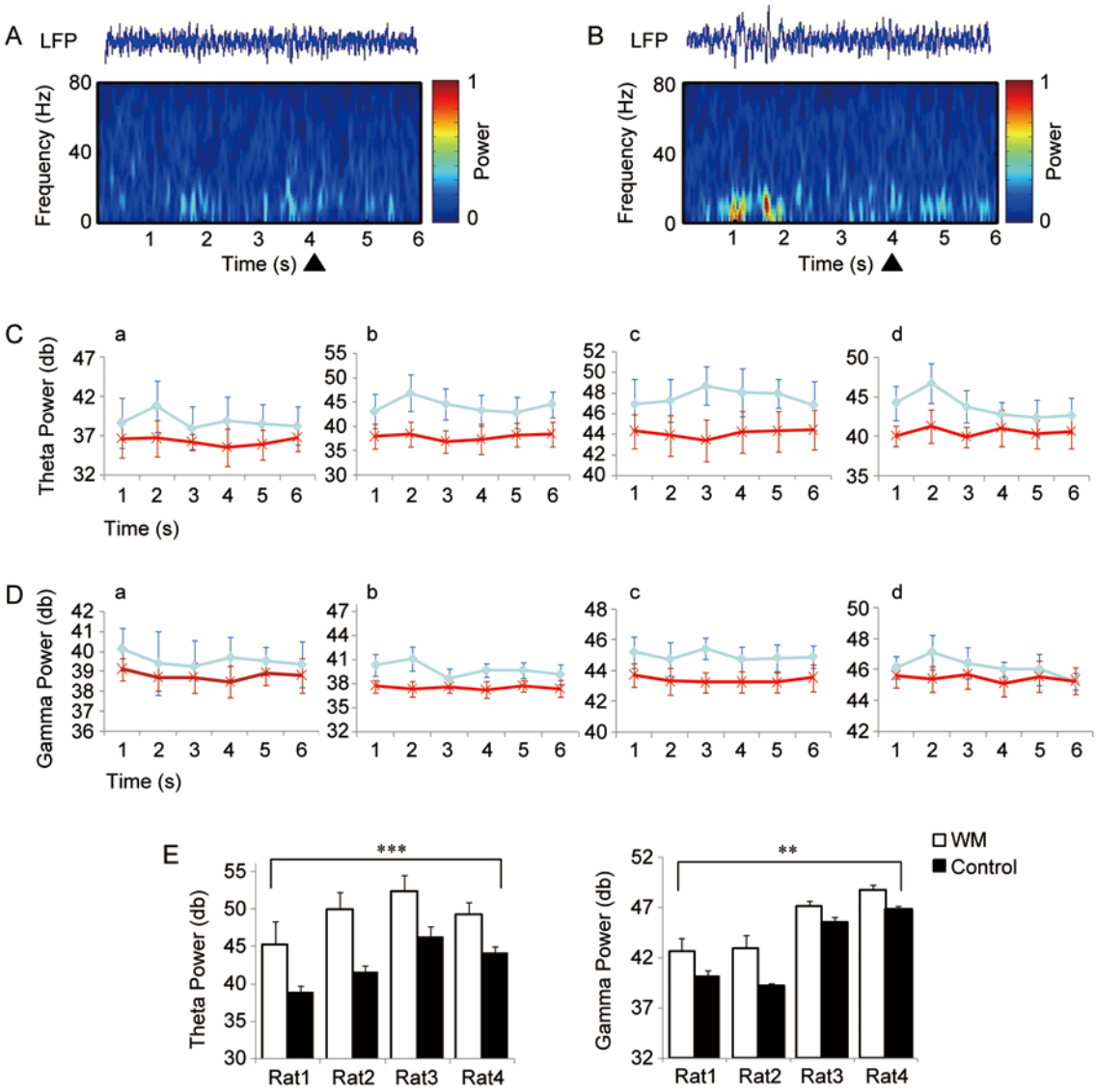

Fig. 5. Comparisons of theta/gamma power between the working memory and control groups. A: An example of LFP and time-frequency representation in control group. B: An example of LFP and time-frequency representation in working memory group. The power was normalized. ▲ denotes the reference point. C: Average theta power of control group (red) and working memory group (blue) in each second. D: Average gamma power of control group (red) and working memory group (blue) in each second. a–d indicate the four rats. E: Theta and gamma power in control and working memory (WM) groups in each second when the LFP power peaked. All data are expressed as mean ± SEM. $^{**}P$ <0.005, $^{***}P$ <0.001 *vs* control group, *t* test.

choice before the rat crossed the corner of the Y maze. We calculated the theta and gamma power in each second for both groups when the LFP power peaked. Group statistics showed that the theta and gamma power in the working memory group were greater than those in the control group in the second when the LFP power of both groups peaked (Fig. 5E, $^{**}P$ <0.005, $^{***}P$ <0.001).

Theta and Gamma Power in Working Memory-Related Features

Spectral analysis showed remarkable power changes at frequencies <30 Hz, and it was difficult to discriminate power changes at frequencies >30 Hz (Fig. 5B). It would be helpful to remove the noise. Moreover, the increased LFP components could not simply be assumed to be completely

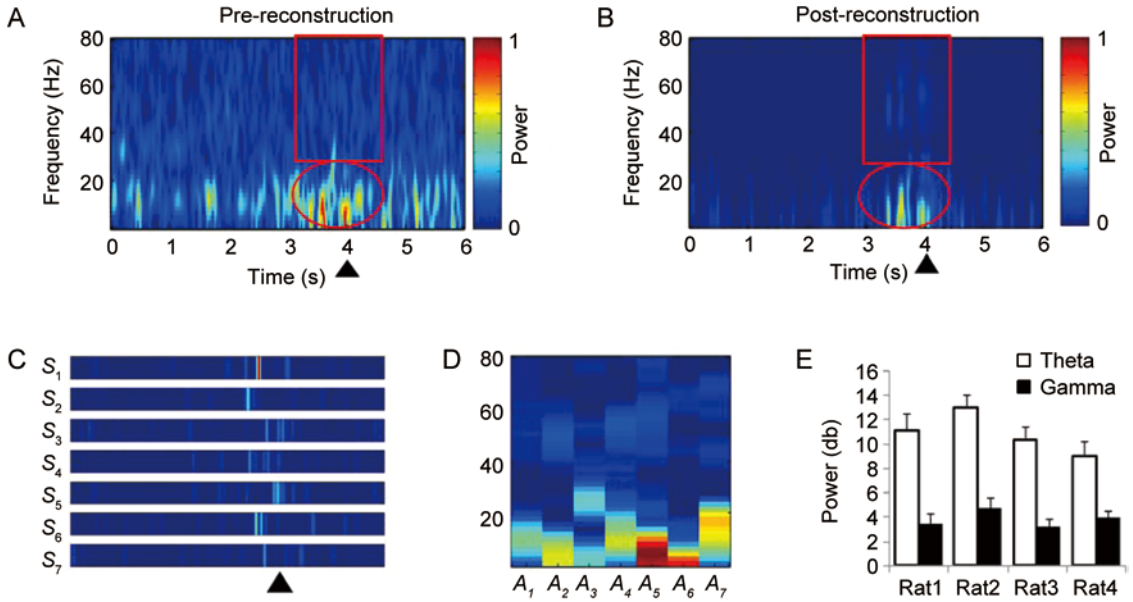

Fig. 6. Results of SNMF and reconstruction for a single channel. A and B: Time-frequency representations before (A) and after (B) reconstruction for a single channel. For ease of comparison, the power is normalized. The time-frequency representation before reconstruction shows more evident power changes in the lower frequencies (<30 Hz) than in the higher frequencies (>30 Hz). C: Sparse vectors corresponding to the time-frequency representation after reconstruction in B. D: Basic vectors corresponding to the time-frequency representation after reconstruction in B. E: Theta and gamma power in working memory-related features. All data are expressed as mean ± SEM. ▲ denotes the reference point.

devoted to encoding working memory. It was necessary to extract the power-increased LFP components.

We constructed the data matrix $X \in R_{+}^{630\times12000}$ (630 = 15 × 42) from 15-channel LFP data, and $X \in R_{+}^{672\times12000}$ (672 = 16 × 42) from 16-channel LFP data. The parameters r and λ were chosen to be 40 and 0.6 respectively after repeated tests. After SNMF, we obtained 50 groups of basis matrix ***A*** and sparse matrix ***S*** from 50 groups of LFP data. Subsequently, we selected working memory-related features one by one and eliminated the noise features. Then we used the inverse operation of SNMF to reconstruct the features. After that, the noise was removed, and only the time-frequency information of working memory-related features remained. The results of SNMF and reconstruction for a single channel are shown in Fig. 6. It was easier to discriminate power changes at frequencies >30 Hz from the time-frequency representation after reconstruction than before (Fig. 6A, B). We calculated the theta and gamma power in working memory-related features for each rat (Fig. 6E) and found they were significantly greater than zero (P < 0.001, t test).

DISCUSSION

As noted above, the column vectors of basis matrix ***A*** could be considered as representing different types of postsynaptic potentials, which correspond to different neuronal activity. The sparseness of postsynaptic activity is the prerequisite assumption for using the SNMF algorithm to extract features from LFPs. The successful feature extraction suggests that postsynaptic activity can be well-simulated by the sparse activity model. The disadvantage of the SNMF algorithm in this study was that the basis matrix ***A*** contained not only the characteristics of the data in the frequency domain, but also information of the channels, which increased the difficulty of analyzing LFP features. However, this problem is avoidable with the sparse non-negative tensor factorization (SNTF) algorithm[27]. So we will use the SNTF algorithm to extract LFP features in the future work.

Our results showed that theta and gamma power were not increased at all times during the working memory task but increased remarkably over controls in a specific

period before the rat crossed the corner of the Y maze. And the theta and gamma power in the power-increased LFP components were significantly greater than zero. These suggest that both the theta and gamma bands are meaningful for working memory. Earlier research has shown that the theta band reflects neuronal resources involved in memory processes and directed attention[28,29]. The increased theta power is probably related to the organization of spatial information and decision-making over delays[30-32] in the Y-maze working memory task. Besides, studies show that the gamma band is involved in perceptual processing, which is associated with the maintenance of detailed item representations over a delay[33,34].

In continuing analyses of cortical LFPs, researchers have shown that the interaction between the frequency bands might reflect a higher-order representation[35]. Theta-gamma coupling is thought to play a role in the maintenance of working memory and sequential memory organization[36]. In this study, we found that theta and gamma band activity often co-existed in the working memory-related basis vectors (such as basis vectors A_2, A_4, A_5, A_6 and A_7 in Fig. 6D), suggesting that there is a power relationship between the theta and gamma bands. However, this still needs further clarification.

ACKNOWLEDGEMENTS

This work was supported by the National Natural Science Foundation of China (61074131 and 91132722) and the Doctoral Fund of the Ministry of Education of China (21101202110007).

Received date: 2012-05-21; Accepted date: 2012-12-17

REFERENCES

[1] Mintzer MZ, Griffiths RR. Differential effects of scopolamine and lorazepam on working memory maintenance versus manipulation processes. Cogn Affect Behav Neurosci 2007, 7: 120–129.

[2] Baddeley AD. Working memory: looking back and looking forward. Nat Rev Neurosci 2003, 4: 829–839.

[3] Lupien SJ, Buss C, Schramek TE. Hormetic influence of glucocorticoids on human memory. Nonlinearity Biol Toxicol Med 2005, 3: 23–56.

[4] Miller EK. An integrative theory of prefrontal cortex. Ann Rev Neurosci 2001, 24: 167–202.

[5] Wang XJ. Synaptic reverberation underlying mnemonic persistent activity. Trends Neurosci 2001, 24: 455–463.

[6] Fuster JM, Bauer RH, Jervey J. Functional interactions between inferotemporal and prefrontal cortex in a cognitive task. Brain Res 1985. 330: 299–307.

[7] Braver TS, Cohen JD, Nystrom LE, Jonides J, Smith EE, Noll DC. A parametric study of prefrontal cortex involvement in human working memory. Neuroimage 1997, 5: 49–62.

[8] Logothetis NK. The underpinnings of the BOLD functional magnetic resonance imaging signal. J Neurosci 2003, 23: 3963–3971.

[9] Pesaran B, Pezaris J, Sahani M, Mitra PP, Andersen RA. Temporal structure in neuronal activity during working memory in macaque parietal cortex. Nat Neurosci 2002, 5: 805–811.

[10] Carsten M, Jörn R, Eilon V, Oliveira SC, Aertsen A, Rotter S. Inference of hand movements from local field potentials in monkey motor cortex. Nat Neurosci 2003, 6: 1253–1254.

[11] Benchenane K, Peyrache A, Khamassi M, Tierney PL, Gioanni Y, Battaglia FP, *et al*. Coherent theta oscillations and reorganization of spike timing in the hippocampal-prefrontal network upon learning. Neuron 2010, 66: 921–936.

[12] Montgomery SM, Buzsaki G. Gamma oscillations dynamically couple hippocampal CA3 and CA1 regions during memory task performance. Proc Natl Acad Sci U S A 2007, 104: 14495–14500.

[13] Driver JE, Racca C, Cunningham MO, Towers SK, Davies CH, Whittington MA, *et al*. Impairment of hippocampal gamma-frequency oscillations *in vitro* in mice overexpressing human amyloid precursor protein (APP). Eur J Neurosci 2007, 26: 1280–1288.

[14] Lisman J. The theta/gamma discrete code occurring during the hippocampal phase precession may be a more general brain coding scheme. Hippocampus 2005, 15: 913–922.

[15] Histed MH, Bonin V, Reid RC. Direct activation of sparse, distributed populations of cortical neurons by electrical microstimulation. Neuron 2009, 63: 508–522.

[16] Joelving FC, Compte A, Constantinidis C. Temporal properties of posterior parietal neuron discharges during working memory and passive viewing. J Neurophysiol 2007, 97: 2254–2266.

[17] Lundqvist M, Herman P, Lansner A. Theta and Gamma power increases and Alpha/Beta power decreases with memory load in an attractor network model. J Cogn Neurosci 2011, 23: 3008–3020.

[18] Siegel M, Warden MR, Miller EK. Phase-dependent neuronal coding of objects in short-term memory. Proc Natl Acad Sci U S A 2009, 106: 21341–21346.

[19] Fujisawa S, Buzsáki G. A 4 Hz oscillation adaptively synchronizes prefrontal, vta, and hippocampal activities.

Neuron 2011, 72: 153–165.

[20] Olshausen BA, Field DJ. Emergence of simple-cell receptive field properties by learning a sparse code for natural images. Nature 1996, 381: 607–609.

[21] Kim H, Park H. Sparse non-negative matrix factorizations via alternating non-negativity-constrained least squares for microarray data analysis. Bioinformatics 2007, 23: 1495–1502.

[22] Hoyer PO. Nonnegative matrix factorization with sparseness constraints. J Mach Learn Res 2004, 5: 1457–1469.

[23] Lee DD, Seung HS. Algorithms for non-negative matrix factorization. Adv Neural Inf Process Syst 2001, 13: 556–562.

[24] Shi JL, Luo ZG. Research on the Advances of nonnegative matrix factorization and its application in bioinformatics. Comput Eng Sci 2010, 32: 117–123.

[25] Kim PM, Tidor B. Subsystem identification through dimensionality reduction of large-scale gene expression data. Genome Res 2003, 13: 1706–1718.

[26] Monti S, Tamayo P, Mesirov J, Golub T. Consensus clustering: A resampling based method for class discovery and visualization of gene expression microarray data. Mach Learn 2003, 52: 91–118.

[27] Hazan T, Polak S, Shashua A. Sparse image coding using a 3D nonnegative tensor factorization. IEEE ICCV 2005, 1: 50–57.

[28] Raqhavachari S, Lisman JE, Tully M, Madsen JR, Bromfield EB, Kahana MJ. Theta oscillations in human cortex during a working-memory task: evidence for local generators. J Neurophysiol 2006, 95: 1630–1638.

[29] Missonnier P, Gold G, Herrmann FR, Fazio-Costa L, Michel JP, Deiber MP, *et al*. Decreased theta event-related synchronization during working memory activation is associated with progressive mild cognitive impairment. Dement Geriatr Cogn Disord 2006, 22: 250–259.

[30] Hyman JM, Hasselmo ME, Seaman JK. What is the functional relevance of prefrontal cortex entrainment to hippocampal theta rhythms? Front Neurosci 2011, 5: 24.

[31] Jones MW, Wilson MA. Theta rhythms coordinate hippocampal - prefrontal interactions in a spatial memory task. PLoS Biol 2005, 3: 2187–2199.

[32] Raghavachari S, Kahana MJ, Rizzuto DS, Caplan JB, Kirschen MP, Bourgeois B, *et al*. Gating of human theta oscillations by a working memory task. J Neurosci 2001, 21: 3175–3183.

[33] Howard MW, Rizzuto DS, Caplan JB, Madsen JR, Lisman J, Aschenbrenner-Scheibe R, *et al*. Gamma oscillations correlate with working memory load in humans. Cereb Cortex 2003, 13: 1369–1374.

[34] Herrmann CS, Munk MH, Engel AK. Cognitive functions of gamma-band activity: memory match and utilization. Trends Cogn Sci 2004, 8: 347–355.

[35] Sejnowski TJ, Destexhe A. Why do we sleep? Brain Res 2000, 886: 208–223.

[36] Canolty RT, Edwards E, Dalal SS, Soltani M, Nagarajan SS, Kirsch HE, *et al*. High gamma power is phase locked to theta oscillations in human neocortex. Science 2006, 313: 1626–1628.